Acta Crystallographica Section B
Structural Science
ISSN 0108-7681

Hydrated metal complexes of *N*-(6-amino-3,4-dihydro-3-methyl-5-nitroso-4-oxopyrimidin-2-yl)glycinate: interplay of molecular, molecular–electronic and supramolecular structures

John N. Low,[a]† Jose M. Moreno Sánchez,[b] Paloma Arranz Mascarós,[c] M. Luz Godino Salido,[c] Rafael López Garzon,[c] Justo Cobo Domingo[c] and Christopher Glidewell[d]*

[a]Department of Chemistry, University of Aberdeen, Meston Walk, Old Aberdeen AB24 3UE, Scotland, [b]Departamento de Química Inorgánica, Facultad de Ciencias, Universidad de Granada, 18071 Granada, Spain, [c]Departamento de Química Inorgánica y Orgánica, Universidad de Jaén, 23071 Jaén, Spain, and [d]School of Chemistry, University of St Andrews, St Andrews KY16 9ST, Scotland

† Postal address: Department of Electronic Engineering and Physics, University of Dundee, Nethergate, Dundee DD1 4HN, Scotland.

Correspondence e-mail: cg@st-andrews.ac.uk

Received 27 November 2000
Accepted 12 December 2000

The title anion, $(C_7H_8N_5O_4)^-$, L^-, forms hydrated metal complexes with a range of metal ions M^+ and M^{2+}. Lithium and manganese(II) form finite molecular aggregates $[Li(L)(H_2O)_3]$ (1) and $[Mn(L)_2(H_2O)_4].6H_2O$ (4) in which the molecular aggregates are linked into three-dimensional frameworks by extensive hydrogen bonding. The sodium and potassium derivatives, $[Na_2(L)_2(H_2O)_3]$ (2) and $[K(L)(H_2O)]$ (3) both form organic–inorganic hybrid sheets in which metal–oxygen ribbons are linked by strips containing only organic ligands: these sheets are linked by hydrogen bonds into three-dimensional frameworks. In (2) the metal–oxygen ribbon is built from pairs of edge-shared trigonal bipyramids linked by water molecules, while in (3) it consists of a continuous chain of vertex-sharing octahedra. The nitroso group in the anion acts as an η^1 ligand towards Na^+ and as an η^2 ligand towards K^+. In all cases the anion L^- shows the same unusual pattern of interatomic distances as the neutral parent *L*H.

1. Introduction

We have recently discussed the interplay of molecular, molecular–electronic and supramolecular structures in the *N*-(6-amino-3,4-dihydro-3-methyl-5-nitroso-4-oxopyrimidin-2-yl) derivatives (I) of a range of amino acids (Low *et al.*, 2000). The structures of these compounds are characterized (*a*) by very short intermolecular O—H···O hydrogen bonds, with O···O distances generally less than 2.50 Å, typical of ionic O—H···O$^-$ hydrogen bonds even though the compounds (I) all consist of neutral molecules; and (*b*) by highly unusual intramolecular bond distances. An interpretation of the relationship between the intramolecular dimensions and the very short hydrogen bonds was proposed on the basis of database analysis and computational modelling.

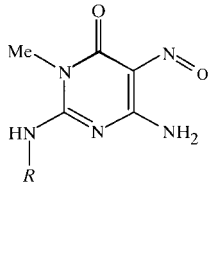

(I) (*a*) $R = CH_2COOH$
(*b*) $R = CH(COOH)CH_2CH_2SMe$
(*c*) $R = CH(COOH)CHMe_2$
(*d*) $R = CH(COOH)CH_2OH$
(*e*) $R = CH(COOH)CH(OH)Me$

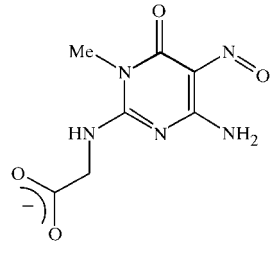

L^-

© 2001 International Union of Crystallography
Printed in Great Britain – all rights reserved

Table 1
Experimental details.

	(1)	(2)	(3)	(4)
Crystal data				
Chemical formula	$C_7H_{14}LiN_5O_7$	$C_{14}H_{22}N_{10}Na_2O_{11}$	$C_7H_{10}KN_5O_5$	$C_{14}H_{24}MnN_{10}O_{12}\cdot 6H_2O$
Chemical formula weight	287.17	552.4	283.3	687.46
Cell setting, space group	Monoclinic, C_2/c	Triclinic, $P\overline{1}$	Monoclinic, $P2_1/c$	Triclinic, $P\overline{1}$
a, b, c (Å)	24.7736 (6), 7.6525 (3), 14.0096 (5)	7.5702 (1), 11.5237 (2), 13.3743 (3)	7.8114 (2), 16.4811 (5), 8.5560 (2)	7.4476 (3), 8.2351 (4), 12.6372 (5)
α, β, γ (°)	90, 114.3751 (13), 90	104.4350 (8), 97.8415 (8), 103.5004 (7)	90, 100.408 (2), 90	105.258 (2), 92.153 (3), 108.94 (2)
V (Å^3)	2419.20 (14)	1074.95 (3)	1083.38 (5)	700.81 (5)
Z	8	2	4	1
D_x (Mg m^{-3})	1.577	1.707	1.737	1.629
Radiation type	Mo $K\alpha$	Mo $K\alpha$	Mo $K\alpha$	Mo $K\alpha$
No. of reflections for cell parameters	2637	5449	2814	3131
θ range (°)	2.95–27.46	2.93–29.0	2.93–29.0	1.69–27.47
μ (mm^{-1})	0.138	0.179	0.516	0.569
Temperature (K)	150.0 (1)	150 (2)	150 (2)	150 (2)
Crystal form, colour	Block, red	Plate, colourless	Block, red	Plate, red
Crystal size (mm)	0.20 × 0.10 × 0.10	0.45 × 0.25 × 0.05	0.10 × 0.10 × 0.05	0.45 × 0.35 × 0.08
Data collection				
Diffractometer	Kappa-CCD	Kappa-CCD	Kappa-CCD	Kappa-CCD
Data collection method	φ and ω scans with κ offsets	φ and ω scans with κ offsets	φ and ω scans with κ offsets	φ and ω scans with κ offsets
Absorption correction†	Multi-scan	Multi-scan	Multi-scan	Multi-scan
T_{min}	0.9729	0.9239	0.9502	0.7840
T_{max}	0.9863	0.9911	0.9747	0.9586
No. of measured, independent and observed parameters	7232, 2637, 2024	15 704, 5449, 4455	8482, 2814, 2226	7489, 3131, 2814
Criterion for observed reflections	$I > 2\sigma(I)$	$I > 2\sigma(I)$	$I > 2\sigma(I)$	$I > 2\sigma(I)$
R_{int}	0.027	0.053	0.046	0.068
θ_{max} (°)	27.46	29.00	29.00	27.47
Range of h, k, l	$-32 \rightarrow h \rightarrow 32$ $-9 \rightarrow k \rightarrow 9$ $-18 \rightarrow l \rightarrow 18$	$-9 \rightarrow h \rightarrow 10$ $-15 \rightarrow k \rightarrow 15$ $-16 \rightarrow l \rightarrow 18$	$-10 \rightarrow h \rightarrow 10$ $-19 \rightarrow k \rightarrow 23$ $-11 \rightarrow l \rightarrow 11$	$-9 \rightarrow h \rightarrow 9$ $-10 \rightarrow k \rightarrow 10$ $-15 \rightarrow l \rightarrow 16$
Refinement				
Refinement on	F^2	F^2	F^2	F^2
$R[F^2>2\sigma(F^2)]$, $wR(F^2)$, S	0.0449, 0.1214, 1.032	0.0468, 0.1362, 1.041	0.0416, 0.1079, 1.072	0.04, 0.1066, 1.097
No. of reflections and parameters used in refinement	2637, 200	5449, 354	2814, 170	3131, 233
H-atom treatment	H-atom parameters constrained	H-atom parameters constrained	H-atom parameters constrained	H-atom parameters constrained
Weighting scheme	$w = 1/[\sigma^2(F_o^2) + (0.0621P)^2 + 0.6971P]$, where $P = (F_o^2 + 2F_c^2)/3$	$w = 1/[\sigma^2(F_o^2) + (0.0761P)^2 + 0.2718P]$, where $P = (F_o^2 + 2F_c^2)/3$	$w = 1/[\sigma^2(F_o^2) + (0.0520P)^2 + 0.1977P]$, where $P = (F_o^2 + 2F_c^2)/3$	$w = 1/[\sigma^2(F_o^2) + (0.0452P)^2 + 0.4451P]$, where $P = (F_o^2 + 2F_c^2)/3$
$(\Delta/\sigma)_{max}$	0.001	0.000	0.001	0.006
$\Delta\rho_{max}$, $\Delta\rho_{min}$ (e Å^{-3})	0.241, −0.302	0.347, −0.453	0.344, −0.500	0.499, −0.570

Computer programs used: *Kappa-CCD Server Software* (Nonius, 1997), *DENZO* (Otwinowski & Minor, 1997), *SHELXS*97 (Sheldrick, 1997*a*), *SHELXL*97 (Sheldrick, 1997*b*), *PLATON* (Spek, 2000), *WordPerfect* macro *PRPKAPPA* (Ferguson, 1999), *ORTEP*II (Johnson, 1976). † Blessing (1995, 1997).

Developing this study, we have now investigated some metal derivatives containing the anionic ligand L^- derived from the 2-pyrimidinylglycine derivative LH = (I*a*) and here we discuss the structures of hydrated complexes of this ligand with Li (1), Na (2), K (3) and Mn(II) (4), all of which prove to have the ligand L^- bonded directly to the metal. By contrast, the Mg and Zn analogues (5) and (6), respectively, whose structures have been reported previously (Arranz Mascarós *et al.*, 1999, 2000), are both salts containing the hexa-aqua metal cations $[M(H_2O)_6]^{2+}$, with no direct interaction between L^- and the metals.

2. Experimental

2.1. Synthesis

The neutral compound LH was prepared according to the reported method (Low *et al.*, 1997) and the corresponding ammonium salt $[NH_4]^+L^-$ was obtained by addition of ammonia to an aqueous solution of LH. Compounds (1)–(3) were prepared by the addition of the corresponding amount of the metal chloride (LiCl, NaCl or KCl) to a stirred aqueous solution of $[NH_4]^+L^-$. Metal:ligand molar ratios of 4:1 were used for (1) and (3) and a ratio of 1:1 for (2). The resulting solutions were left to evaporate at atmospheric pressure over

Table 2
Metal coordination geometry for (1)–(4) (Å, °).

(1)			
Li1—O1	1.986 (3)	Li1—O3	1.959 (3)
Li1—O2	1.933 (3)	Li1—O21	1.934 (3)
O1—Li1—O2	103.6 (2)	O1—Li1—O21	122.5 (2)
O2—Li1—O3	111.9 (2)	O2—Li1—O21	105.9 (2)
O3—Li1—O1	108.3 (2)	O3—Li1—O2	1104.7 (2)
(2)			
Na1—O1	2.476 (2)	Na2—O1	2.404 (2)
Na1—O2	2.366 (2)	Na2—O3	2.325 (2)
Na1—O21*A*	2.273 (2)	Na2—O21*B*	2.369 (2)
Na1—O5*A*^{i}	2.359 (2)	Na2—O5*B*^{ii}	2.427 (2)
Na1—O21*A*^{iii}	2.492 (2)	Na2—O21*B*^{iv}	2.359 (2)
O1—Na1—O21*A*^{iii}	153.04 (4)	O1—Na2—O21*B*^{iv}	151.85 (5)
O1—Na1—O2	78.62 (4)	O1—Na2—O3	85.44 (5)
O1—Na1—O21*A*	110.28 (4)	O1—Na2—O21*B*	90.38 (4)
O1—Na1—O5*A*^{i}	108.96 (4)	O1—Na2—O5*B*^{ii}	80.27 (4)
O2—Na1—O21*A*	126.48 (4)	O3—Na2—O21*B*	119.87 (4)
O21*A*—Na1—O5*A*^{i}	131.98 (4)	O21*B*—Na2—O5*B*^{iii}	121.43 (4)
O5*A*^{i}—Na1—O2	87.51 (4)	O5*B*^{ii}—Na2—O3	116.79 (4)
O21*A*^{iii}—Na1—O2	76.14 (4)	O21*B*^{iv}—Na2—O3	122.66 (5)
O21*A*^{iii}—Na1—O21*A*	78.14 (4)	O21*B*^{iv}—Na2—O21*B*	77.35 (4)
O21*A*^{iii}—Na1—O5*A*^{i}	79.36 (4)	O21*B*^{iv}—Na2—O5*B*^{ii}	84.70 (4)
(3)			
K1—O1	2.762 (2)	K1—O4^{v}	2.762 (2)
K1—O1^{vi}	2.811 (2)	K1—N5^{vii}	3.016 (2)
K1—O21	2.779 (2)	K1—O5^{vii}	3.132 (2)
K1—O21^{viii}	2.748 (2)	K1—*X*^{vii}	3.005 (2)†
O4^{v}—K1—O1	76.55 (4)	*X*^{vii}—K1—O1	97.16 (4)
O4^{v}—K1—O1^{vi}	75.90 (4)	*X*^{vii}—K1—O1^{vi}	62.84 (4)
O4^{v}—K1—O21	100.44 (4)	*X*^{vii}—K1—O2	189.53 (4)
O4^{v}—K1—O21^{viii}	121.03 (4)	*X*^{vii}—K1—O21^{viii}	101.28 (4)
O1—K1—O21^{viii}	73.49 (4)	O1—K1—O21	173.01 (4)
O21^{viii}—K1—O21	103.28 (4)	O1^{vi}—K1—O21^{viii}	163.04 (4)
O21—K1—O1^{vi}	72.27 (4)	O4^{v}—K1—*X*^{vii}	132.17 (4)
O1^{vi}—K1—O1	112.63 (5)		
(4)			
Mn1—O1*W*	2.149 (2)	Mn1—O21	2.156 (2)
Mn1—O2*W*	2.225 (2)		
O21—Mn1—O1*W*	88.16 (5)	O1*W*—Mn1—O2*W*	87.15 (6)
O21—Mn1—O2*W*	86.28 (5)		

Symmetry codes: (i) $-1+x,-1+y,z$; (ii) $1+x,1+y,z$; (iii) $-x,-y,1-z$; (iv) $1-x,-y,2-z$; (v) $1-x,1-y,1-z$; (vi) $x,\frac{1}{2}-y,-\frac{1}{2}+z$; (vii) $1-x,-\frac{1}{2}+y,\frac{3}{2}-z$; (viii) $x,\frac{1}{2}-y,\frac{1}{2}+z$. † *X* is the mid-point of the N5—O5 bond.

several days, producing red crystalline products: triaqua-*N*-(6-amino-3,4-dihydro-3-methyl-5-nitroso-4-oxopyrimidine-2-yl)-glycinatolithium (1); elemental analysis: found C 29.4, H 5.3, N 24.1; $C_7H_{14}LiN_5O_7$ requires C 29.3, H 4.9, N 24.4%; triaqua-bis[*N*-(6-amino-3,4-dihydro-3-methyl-5-nitroso-4-oxopyrimidin-2-yl)glycinato]disodium (2); elemental analysis: found, C 30.5, H 4.2, N 25.5; $C_{14}H_{22}N_{10}Na_2O_{11}$ requires C 30.4, H 4.0, N 25.4%; aqua-*N*-(6-amino-3,4-dihydro-3-methyl-5-nitroso-4-oxopyrimidin-2-yl)glycinatopotassium (3); elemental analysis: found C 29.7, H 3.9, N 24.7; $C_7H_{10}KN_5O_5$ requires C 29.7, H 3.6, N 24.7%. Compound (4) was prepared by mixing aqueous solutions of K^+L^- and $MnCl_2$ to give a ligand:metal ratio of 2:1. The resulting solution was left to evaporate in air until the appearance of a crystalline solid tetraaqua-bis[*N*-(6-amino-3,4-dihydro-3-methyl-5-nitroso-4-oxopyrimidin-2-yl)glycinato]manganese(II) hexahydrate (4), which, once separated by filtration, degraded rapidly in air to afford the amorphous tetraaqua-bis[*N*-(6-amino-3,4-dihydro-3-methyl-5-nitroso-4-oxopyrimidin-2-yl)glycinato]manganese(II) (4*a*). Analysis for (4*a*): found C 29.1, H 4.1, N 23.7; $C_{14}H_{24}MnN_{10}O_{12}$ ($MnL_2{\cdot}4H_2O$) requires C 29.1, H 4.2, N 24.2%; a satisfactory analysis for (4) could not be achieved because of its very ready loss of water.

Crystals of (1)–(3) suitable for single-crystal X-ray diffraction were selected directly from all the analytical samples. Crystals of (4) were kept in a Lindeman capillary surrounded by the mother liquors.

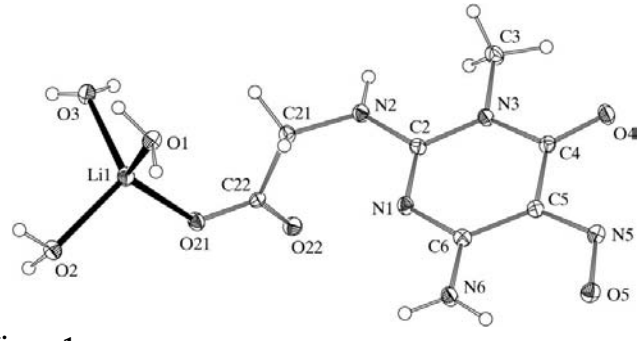

Figure 1
The molecular components of (1), showing the atom-labelling scheme. Displacement ellipsoids are drawn at the 30% probability level.

2.2. Data collection, structure solution and refinement

Details of cell data, data collection and structure solution and refinement are summarized in Table 1.[1] For (1) the systematic absences permitted the space groups *C*2/*c* or *Cc*: *C*2/*c* was selected and confirmed by the successful structure solution and refinement. Compounds (2) and (4) are triclinic: in each case the space group $P\bar{1}$ was chosen and confirmed by the successful structure solution and refinement. For (3) the space group $P2_1/c$ was uniquely assigned from the systematic absences.

The structures were all solved by direct methods using *SHELXS*97 (Sheldrick, 1997*a*) and refined on F^2 with all data using *SHELXL*97 (Sheldrick, 1997*b*). A weighting scheme based upon $P = [F_o^2 + 2F_c^2]/3$ was employed in order to reduce statistical bias (Wilson, 1976). All H atoms were located from difference maps and all were included in the refinements as riding atoms. Those in the organic ligands had N—H 0.88 Å and C—H 0.98 Å (CH_3) or 0.99 Å (CH_2). In the water molecules the O—H distances were constrained to 0.960 (5) Å, and the H—O—H angles were set to 108° by means of an H···H distance constraint of 1.550 (5) Å.

The diagrams were prepared with the aid of *PLATON* (Spek, 2000). Figs. 1–4 show the asymmetric units of (1)–(4) with the atom-labelling schemes: Figs. 5–18 show aspects of the crystal structures. Selected molecular dimensions are given in Tables 2 and 3, and details of the hydrogen bonding are given in Table 4. The structures of compounds for comparison with

[1] Supplementary data for this paper are available from the IUCr electronic archives (Reference: NA0116). Services for accessing these data are described at the back of the journal.

Table 3
Selected intra-anion distances for (I*a*) and (1)–(6) (Å).

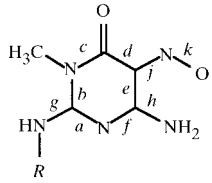

R	*M*	*a*	*b*	*c*	*d*	*e*	*f*	*g*	*h*	*j*	*k*
CH_2COOH	– (I*a*)	1.323 (3)	1.376 (3)	1.381 (3)	1.469 (3)	1.444 (3)	1.332 (3)	1.319 (3)	1.331 (3)	1.316 (3)	1.296 (3)
CH_2COO^-	Li^+ (1)	1.329 (2)	1.381 (2)	1.393 (2)	1.453 (2)	1.446 (2)	1.341 (2)	1.329 (2)	1.318 (2)	1.341 (2)	1.290(2)
CH_2COO^-	Na^+ (2)	1.330 (2)	1.383 (2)	1.395 (2)	1.454 (2)	1.444 (2)	1.341 (2)	1.325 (2)	1.319 (2)	1.331 (2)	1.282 (2)
		1.331 (2)	1.379 (2)	1.398 (2)	1.454 (2)	1.439 (2)	1.339 (2)	1.332 (2)	1.320 (2)	1.333 (2)	1.283 (2)
CH_2COO^-	K^+ (3)	1.331 (2)	1.375 (2)	1.398 (2)	1.453 (2)	1.447 (2)	1.342 (2)	1.329 (2)	1.314 (2)	1.336 (2)	1.295 (2)
CH_2COO^-	Mn^{2+} (4)	1.329 (2)	1.380 (2)	1.392 (2)	1.449 (3)	1.444 (2)	1.344 (2)	1.327 (2)	1.315 (2)	1.339 (2)	1.285 (2)
CH_2COO^-	Mg^{2+} (5)	1.321 (2)	1.385 (2)	1.391 (2)	1.451 (2)	1.447 (2)	1.342 (2)	1.330 (2)	1.314 (2)	1.346 (2)	1.280 (2)
CH_2COO^-	Zn^{2+} (6)	1.325 (2)	1.377 (2)	1.397 (2)	1.450 (2)	1.445 (2)	1.346 (2)	1.335 (2)	1.311 (2)	1.338 (2)	1.290 (2)

those reported here were mainly located using the Cambridge Structural Database (CSD; Allen & Kennard, 1993).

3. Results and discussion

3.1. Syntheses and composition

Compounds (1)–(4) were all readily synthesized by reaction of the ammonium [for (1)–(3)] or potassium [for (4)] salts of L^- with the appropriate metal chlorides in aqueous solution.

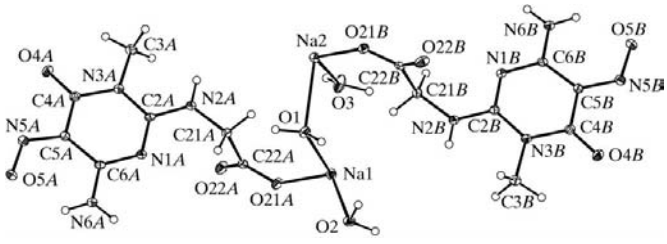

Figure 2
The molecular components of (2), showing the atom-labelling scheme. Displacement ellipsoids are drawn at the 30% probability level.

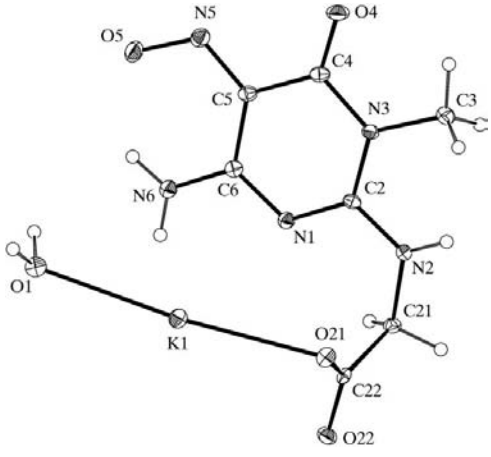

Figure 3
The molecular components of (3), showing the atom-labelling scheme. Displacement ellipsoids are drawn at the 30% probability level.

For the monopositive cations Li^+, Na^+ and K^+, the resulting crystalline products contained one L^- per cation, as expected, while for the dipositive Mn^{2+}, as for Mg^{2+} and Zn^{2+} (Arranz Mascarós *et al.*, 1999, 2000), there are two L^- per cation. The unexpected and unpredictable aspect of the compositions of (1)–(6) is the wide variation in the degree of hydration in each compound. Thus, for the Group 1 derivatives, (1)–(3) contain, respectively, 3, 1.5 and 1 molecule of water per cation, while for Mn^{2+} there exist both a crystalline decahydrate (4) and, in addition, a tetrahydrate (4*a*) characterized so far only by elemental analysis, which proved to be amorphous to X-rays. The Mg^{2+} and Zn^{2+} compounds (5) and (6) both crystallize as octahydrates.

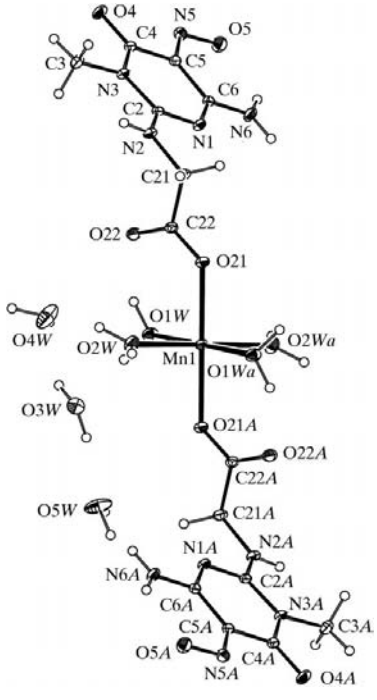

Figure 4
The molecular components of (4), showing the atom-labelling scheme. Displacement ellipsoids are drawn at the 30% probability level. The atoms marked '*a*' are at the symmetry position $(1-x, -y, 1-z)$.

Table 4
Hydrogen-bond geometry for (1)–(4) (Å, °).

	H···*A*	*D*···*A*	*D*—H···*A*	Motif	Direction
(1)					
N2—H2···O2^{i}	2.14	2.918 (2)	146	*C*(7) translation	[010]
N6—H6*A*···O4^{ii}	2.14	2.925 (2)	148	*C*(6) translation	[010]
N6—H6*B*···O5	1.98	2.627 (2)	129	*S*(6)	–
O1—H11···O22^{iii}	1.80 (2)	2.746 (2)	167 (2)	*C*(6) zigzag	[001]
O1—H12···O4^{iv}	2.08 (2)	2.945 (2)	148 (2)	*C*(11) spiral	[010]
O2—H21···O3^{v}	1.90 (2)	2.844 (2)	171(2)	*C*(4) spiral	[010]
O2—H22···O21^{vi}	1.75 (2)	2.697 (2)	171 (2)	$R_2^2(8)$	–
O3—H31···O22^{vii}	1.77 (2)	2.726 (2)	176 (2)	$R_2^2(12)$	–
O3—H32···O5^{viii}	1.74 (2)	2.692 (2)	175 (2)	*C*(13) translation	[110]
(2)					
N2*A*—H2*A*···O2^{ix}	2.05	2.810 (2)	144	*C*(7) translation	[100]
N2*B*—H2*B*···O21*B*^{x}	2.43	3.187 (2)	144	$R_2^2(8)$	–
N6*A*—H6*A*1···O4*A*^{xi}	2.13	3.002 (2)	169	*C*(6) translation	[100]
N6*A*—H6*A*2···O5*A*	1.99	2.628 (2)	128	*S*(6)	–
N6*B*—H6*B*1···O4*B*^{ix}	2.09	2.953 (2)	165	*C*(6) translation	[100]
N6*B*—H6*B*2···O5*B*	1.98	2.628 (2)	129	*S*(6)	–
O1—H11···O22*B*^{x}	1.77 (2)	2.711 (2)	166 (2)	$R_2^2(12)$	–
O1—H12···N5*B*^{xii}	1.89 (2)	2.738 (2)	146 (2)	*C*(12) translation	[110]
O2—H21···O22*A*^{xiii}	1.76 (2)	2.691 (2)	161 (2)	$R_2^2(12)$	–
O2—H22···O22*B*^{x}	1.827 (7)	2.751 (2)	161 (2)	$R_2^2(16)$	–
O3—H31···N5*A*^{xiv}	1.87 (2)	2.771 (2)	156 (2)	*C*(14) translation	[110]
O3—H32···O22*A*^{xv}	1.75 (2)	2.708 (2)	175 (2)	$R_2^2(16)$	–
(3)					
N2—H2···O22^{xvi}	2.03	2.796 (2)	144	*C*(5) zigzag	[001]
N6—H6*A*···O21^{xvii}	2.02	2.872 (2)	162	*C*(9) zigzag	[001]
N6—H6*B*···O5	1.95	2.605 (2)	130	*S*(6)	–
O1—H11···O22^{xviii}	1.796 (7)	2.754 (2)	177 (2)	*C*(6) zigzag	[201]
O1—H12···O5^{xix}	1.83 (2)	2.761 (2)	164 (2)	$R_2^2(26)$	-
(4)					
N2—H2···O3*W*^{xiii}	2.02	2.804 (2)	148	$R_4^4(18)$	–
N6—H6*A*···O4^{ix}	2.00	2.827 (2)	156	*C*(6) translation	[100]
N6—H6*B*···O5	1.97	2.620 (2)	130	*S*(6)	–
O1*W*—H1*W*1···O22	1.86 (2)	2.742 (2)	151 (2)	*S*(6)	–
O1*W*—H2*W*1···O3*W*	1.77 (2)	2.731 (2)	177 (2)	*D*	–
O2*W*—H1*W*2···O22^{xiii}	1.98 (2)	2.933 (2)	174 (2)	$R_2^2(12)$	–
O2*W*—H2*W*2···O5^{xx}	1.80 (2)	2.705 (2)	156 (2)	*C*(13) translation	[011]
O3*W*—H1*W*3···O5*W*	1.88 (3)	2.817 (3)	167 (3)	*D*	–
O3*W*—H2*W*3···O4*W*	2.00 (3)	2.865 (3)	150 (3)	*D*	–
O4*W*—H1*W*4···O4*W*^{xxi}	1.85 (3)	2.754 (3)	158 (4)	$R_2^2(4)$	–
O4*W*—H2*W*4···O21^{xxii}	2.05 (2)	2.981 (3)	164 (3)	$C_3^3(8)$	[010]
O5*W*—H1*W*5···O4^{xxiii}	2.19 (2)	2.958 (2)	137 (2)	$C_3^3(15)$	[10$\bar{1}$]
O5*W*—H1*W*5···N5^{xxiii}	2.24 (2)	3.100 (3)	148 (2)	$C_3^3(16)$	[10$\bar{1}$]
O5*W*—H2*W*5···O22^{xxiv}	1.92 (2)	2.864 (2)	167 (2)	$R_6^6(30)$	-

Symmetry codes: (i) $x, 1+y, z$; (ii) $x, -1+y, z$; (iii) $x, 1-y, \frac{1}{2}+z$; (iv) $1-x, -1+y, \frac{1}{2}-z$; (v) $\frac{1}{2}-x, -\frac{1}{2}+y, \frac{1}{2}-z$; (vi) $\frac{1}{2}-x, \frac{1}{2}-y, -z$; (vii) $\frac{1}{2}-x, \frac{3}{2}-y, -z$; (viii) $-\frac{1}{2}+x, -\frac{1}{2}+y, z$; (ix) $1+x, y, z$; (x) $-x, -y, 2-z$; (xi) $-1+x, y, z$; (xii) $1+x, 1+y, z$; (xiii) $-x, -y, 1-z$; (xiv) $-1+x, -1+y, z$; (xv) $1-x, -y, 1-z$; (xvi) $x, \frac{1}{2}-y, -\frac{1}{2}+z$; (xvii) $x, \frac{1}{2}-y, \frac{1}{2}+z$; (xviii) $1+x, \frac{1}{2}-y, \frac{1}{2}+z$; (xix) $1-x, 1-y, 2-z$; (xx) $x, -1+y, -1+z$; (xxi) $-x, 1-y, 1-z$; (xxii) $x, 1+y, z$; (xxiii) $1+x, y, -1+z$; (xxiv) $1-x, 1-y, 1-z$.

3.2. Metal–ligand coordination

3.2.1. Li complex (1). In (1) the lithium ion is four-coordinate (Fig. 1) and the ligating atoms are three O atoms from the water molecules and the carboxylate O21 atom from the anion L^-. The geometry at Li is slightly irregular with the O—Li—O angles ranging from 103.6 (2) to 122.5 (2)°: the Li—O distances are all closely similar with no significant difference between the bonds to H_2O and that to L^- (Table 2). Tetra-coordination is typical for hydrated lithium salts, although the ligand set can vary, depending on the extent of direct coordination of the anion. Thus, with poorly coordinating anions, the cation $[Li(H_2O)_4]^+$ occurs (NOXBIL: Duda *et al.*, 1997; TIPWOE: Zavalij *et al.*, 1997), while displacement of one (LIEDPA: Helm *et al.*, 1977; DANKOS: Herak *et al.*, 1985), two (LHPHTL: Gonschorek & Kuppers, 1975; TIBWUW: Gack & Klufers, 1996; HIGSUL: Gharbi & Jouini, 1996) or three (LIMALD: Town & Small, 1973; HEFWUK; Muller *et al.*, 1994) water molecules by anionic O ligands has also been observed.

3.2.2. Na complex (2). Not only does (2) have a rather unusual composition, but its asymmetric unit comprises two independent anions, two Na ions and three water molecules, thus precisely reflecting the molecular stoichiometry. Both of the Na centres are five-coordinate (Fig. 5), with Na—O distances in the range 2.273 (2)–2.492 (2) Å, with mean value 2.385 Å: the asymmetric unit has been chosen such that water O1 bridges the two Na ions. Each type of Na is coordinated by two O atoms from carboxylate groups in different anions, two O atoms from water molecules and a nitroso O atom; C-nitroso groups are not common ligands for Na ions and no examples were found in the CSD.

Both types of Na have approximate trigonal bipyramidal geometry with, in each case, the bridging O1 occupying one axial site and a carboxylate O atom occupying the other. The geometry at Na2 is close to idealized trigonal bipyramidal: the O—Na—O angle subtended by the two axial ligands, one an anionic O and the other a water O, is 151.85 (5)° and the sum of the O—Na—O angles subtended by the three equatorial ligands is 358.1°. At Na1 the geometry is less regular: while the angle subtended by the two axial ligands is 153.04 (4)°, the sum of the angles subtended by the equatorial ligands is only 346.0°. This low value may be associated with the presence of a sixth O atom, O3, at a distance of 2.882 (2) Å. This is too long for O3 to be regarded as a component of the primary coordination sphere of Na1, but it is within the sum of the van der Waals radii.

Each Na is coordinated by three O atoms from within the selected asymmetric unit and by two further O atoms, each from a different anion. The water O atoms and the carboxylate O21 atoms from the anions combine with the two types of Na ion to generate chains of planar and centrosymmetric Na_2O_2 rings linked by bridging water molecules (Fig. 6). Atoms Na1 and Na2 at (x, y, z) are ligated by O21*A* at $(-x, -y, 1-z)$ and by O21*B* at $(1-x, -y, 2-z)$, respectively. These interactions, when propagated by inversion and translation, generate a sequence of Na_2O_2 rings containing Na1 and O21*A*, and centred at $(n, 0, n+\frac{1}{2})$ (n = zero or integer) alternating with similar rings containing Na2 and O21*B* centred at $(n+\frac{1}{2}, 0, n+1)$ (n = zero or integer). Adjacent rings in this sequence are linked by the water molecules containing O1, so gener-

ating a continuous ribbon running parallel to the [101] direction. Overall, the metal–oxygen ribbon thus consists of pairs of edge-shared trigonal bipyramids, where the shared edges span axial and equatorial sites, linked by water molecules: a single ribbon runs through each unit cell. Pendent from these [101] ribbons are the nitrosopyrimidine ligands and the nitroso O atoms in one ribbon coordinate to the Na ions in each of two neighbouring ribbons, so that the overall coordination polymer takes the form of a continuous sheet.

Within the Na_2O_2 ring centred at (0, 0, $\frac{1}{2}$) and containing Na1, the anionic components lie at (x, y, z) and $(-x, -y, 1-z)$: the C-nitroso groups in these two anions are coordinated, *via* O5*A*, to Na1 ions at $(1+x, 1+y, z)$ and $(-1-x, -1-y, 1-z)$, respectively. These two Na ions are components of Na_2O_2 rings centred at (1, 1, $\frac{1}{2}$) and (-1, -1, $\frac{1}{2}$), so that propagation of the Na1—O5*A* interactions generates a ribbon of centrosymmetric rings running parallel to the [110] direction (Fig. 7). Similarly, the Na_2O_2 ring containing Na2 and centred at ($\frac{1}{2}$, 0, 1) contains anionic components at (x, y, z) and $(1-x, -y, 2-z)$, whose C-nitroso groups act as ligands, *via* O5*B*, to Na2 ions at $(-1+x, -+y, z)$ and $(2-x, 1-y, 2-z)$, respectively. These Na ions are themselves components of Na_2O_2 rings centred at (-0.5, -1, 1) and (1, $\frac{1}{2}$, 1), respectively, and again a chain of rings running parallel to [110] is generated (Fig. 7). These two independent types of [110] chain, one containing Na1 only and the other containing Na2 only, serve to link each [101] chain to its two immediate neighbours, so producing a continuous two-dimensional array parallel to ($\bar{1}11$).

Penta-coordination of Na^+ by oxygen ligands is very commonly observed, in particular in the complexes formed by the cyclic ether $(CH_2CH_2O)_5$, 15-crown-5, and its many derivatives. However, in all these systems the geometry at sodium is determined primarily by the conformational requirements of the ligating polyether. When there are no such constraints, the geometry at sodium may be expected to be in accord with the predictions of the VSEPR model: thus in the $[Na(thf)_5]^+$ cation (thf = tetrahydrofuran, C_4H_8O; GOSBAR: Longato *et al.*, 1999) the geometry is almost exactly trigonal bipyramidal. When only modest conformational constraints are present, as in $[Na(C22C_5)OClO_3]$ ($C22C_5$ is an N_2O_4 cryptand; JIWSOX: Clarke *et al.*, 1991), almost exact square-pyramidal geometry can be observed.

3.2.3. K complex (3). The asymmetric unit of (3) contains one anion L^-, one K^+ ion and one water molecule (Fig. 3). The K centres are, in fact, approximately octahedral: around each K there is an almost exactly planar, and approximately square, arrangement of two water molecules occupying mutually *cis* sites and two anions, each bonded *via* a carboxylate O21 and also occupying a pair of *cis* sites (Fig. 8). In addition to water O1 and carboxylate O21 at (x, y, z), the symmetry-related ligands to K are O1 at $(x, \frac{1}{2}-y, -\frac{1}{2}+z)$ and O21 at $(x, \frac{1}{2}-y, \frac{1}{2}+z)$. Propagation of these interactions produces a ribbon of K_2O_2 rings, each of which is almost planar, which are fused in a spiro fashion at the K sites. This ribbon runs parallel to the [001] direction and there are two such ribbons running through the unit cell, each generated by one of the glide planes

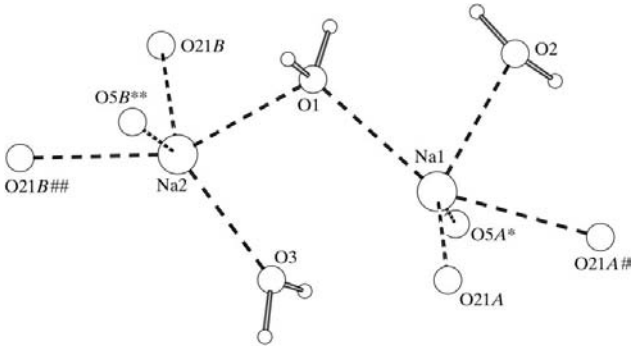

Figure 5
Part of the crystal structure of (2), showing the five-coordination of two independent Na ions. Atoms marked with a single or double star (*) or a single or double hash (#) are at the symmetry positions $(-1+x, -1+y, z)$, $(1+x, 1+y, z)$, $(-x, -y, 1-z)$ and $(1-x, -y, 2-z)$, respectively.

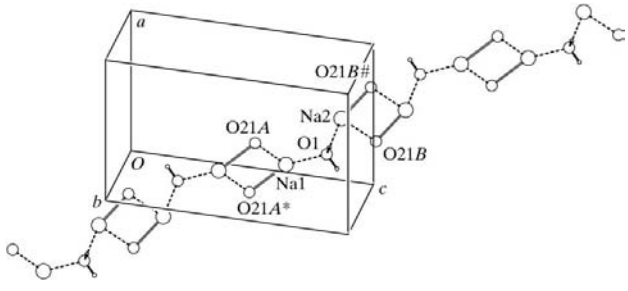

Figure 6
Part of the crystal structure of (2), showing the formation of a [101] chain of Na_2O_2 rings. Atoms marked with a star (*) or hash (#) are at the symmetry positions $(-x, -y, 1-z)$ and $(1-x, -y, 2-z)$, respectively.

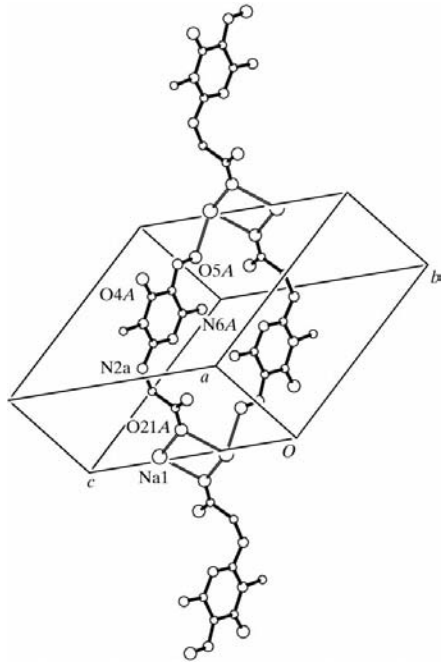

Figure 7
Part of the crystal structure of (2), showing the formation of a [110] ribbon by which the organic ligands link the [101] chains.

in $P2_1/c$ and related to one another by the action of the inversion centres.

The two remaining coordination sites at each K are occupied by O atoms from anions in adjacent ribbons: one site is occupied by an amidic O4 and the other by the nitroso group containing N5 and O5, coordinated to the K in the highly unusual η^2 mode as shown by the almost identical distances K—O5^{i} and K—N5^{i} [(i) $1-x, -\frac{1}{2}+y, \frac{3}{2}-z$; Table 2, Fig. 9], so that in (3) each metal–oxygen ribbon is built from a continuous chain of vertex-shared octahedra. Previously reported structures containing R—N═O ligands bonded to metals in the η^2 mode are rather few in number and all have involved transition metals of the 4*d* or 5*d* series (Pizzotti *et al.*, 1987; Ridouane *et al.*, 1990; Brouwer *et al.*, 1994; Dutta *et al.*, 1997; Skoog & Gladfelter, 1997). The N—O distances in these ligands are all much larger than the 1.295 (2) Å observed here in (3), and they range from 1.386 (3) Å (RUSCOX: Dutta *et al.*, 1997) to 1.432 (6) Å (PIXKEM: Brouwer *et al.*, 1994), consistent with N—O being a single rather than a double bond. In all these cases the ligands are better regarded as dianionic and the complexes themselves as metalla-oxaziridines.

The K site at (x, y, z), which is part of the [001] ribbon generated by the glide plane at y = 0.25, is bonded to the amidic O4 from the anion at $(1-x, 1-y, 1-z)$, which is part of the ribbon generated by the glide plane at y = 0.75. The same K at (x, y, z) is also bonded to the C-nitroso group of the anion at $(1-x, -\frac{1}{2}+y, \frac{3}{2}-z)$, which itself is part of the ribbon generated by the glide plane at y = −0.25. By these means, each [001] ribbon is linked to its two immediate neighbours in the [010] direction, thus producing a continuous sheet parallel to (100).

3.2.4. General comments on the structures of (2) and (3). In both compounds the metal–oxygen ribbons are linked by ribbons of the organic components into sheets: the resulting sheets are thus organic–inorganic hybrids consisting of alternating strips of inorganic metal–oxygen ribbons and organic heterocyclic linkers. In both compounds, these hybrid sheets are further linked by strong hydrogen bonding into continuous three-dimensional frameworks (§3.4).

The overall architecture of these hybrid sheets is thus strongly reminiscent of the architectures observed in hydrated metal 4-nitrophenolates and analogous salts (Minemoto *et al.*, 1992; Sharma *et al.*, 1997; Masse *et al.*, 1999; Muthuraman *et al.*, 1999, 2000), although the metal–oxygen ribbons in these salts are all built from edge-shared MO_6 octahedra. Nearly all of these nitrophenolate salts crystallize in non-centrosymmetric space groups and thus exhibit non-linear optical properties (Masse *et al.*, 1999; Muthuraman *et al.*, 1999). Although (2) and (3) reported here both crystallize in centrosymmetric space groups (Table 1), the presence of the amino acid side chain at N2 provides a very versatile means for the introduction of chirality into the ligand, thus forcing crystallization of the resulting salts in non-centrosymmetric space groups.

3.2.5. Mn^{II} complex (4). In (4) the unique Mn lies on a centre of inversion: it is coordinated by two monodentate L^- ligands in *trans* sites and four water molecules (Fig. 4). The metal coordination in (4) is thus different from that in the Mg and Zn complexes (5) and (6), respectively, where $[M(H_2O)_6]^{2+}$ cations are present with no direct coordination of the ligand L^- to the metal ions. All of the *trans* O—Mn—O angles in (4) are necessarily 180° and none of the *cis* O—Mn—O angles differ from 90° by more than 4° (Table 2). The unique Mn—O(carboxylato) distance is intermediate between the two independent Mn—O(water) distances (Table 2). The mean M—O distances in (4)–(6), in all of which the metal lies at an inversion centre, increase in the order Mg < Zn < Mn. The trend of the mean M—O distances, 2.067, 2.096 and 2.176 Å, respectively, closely reflects that in the ionic radii of six-coordinate M^{2+} ions (high-spin in the case of Mn), 0.72, 0.75 and 0.82 Å, respectively (Shannon & Prewitt, 1970).

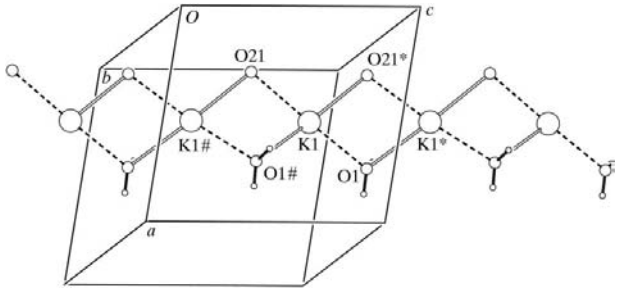

Figure 8
Part of the crystal structure of (3), showing the formation of a ribbon of spiro-linked K_2O_2 rings. Atoms marked with a star (*) or hash (#) are at the symmetry positions $(x, \frac{1}{2}-y, \frac{1}{2}+z)$ and $(x, \frac{1}{2}-y, -\frac{1}{2}+z)$, respectively. Metal–ligand interactions within and between asymmetric units are shown as hollow and dotted lines, respectively.

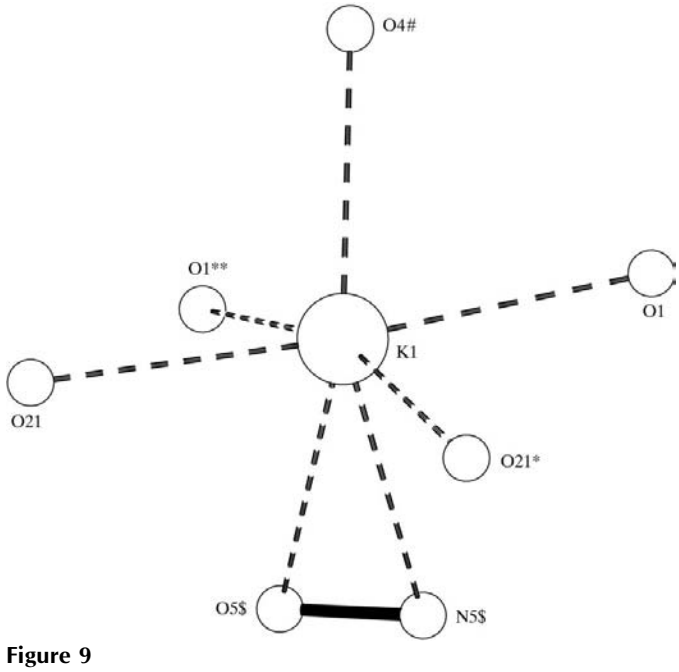

Figure 9
Part of the crystal structure of (3), showing the coordination geometry around K, including atoms N5 and O5 of the η^2 nitroso ligand. Atoms marked with a single star (*), double star (**), hash (#) or dollar sign ($) are at the symmetry positions $(x, \frac{1}{2}-y, \frac{1}{2}+z)$, $(x, \frac{1}{2}-y, -\frac{1}{2}+z)$, $(1-x, 1-y, 1-z)$ and $(1-x, -\frac{1}{2}+y, \frac{3}{2}-z)$, respectively.

The composition of (4), $MnL_2{\cdot}10H_2O$, means that there are six water molecules per Mn, three of which are independent, which are not directly bonded to the metal. While the choice of asymmetric unit is somewhat arbitrary where there are so many independent molecular components, that selected here (Fig. 4) emphasizes that all the water molecules are closely linked by hydrogen bonds, and all play a role in the overall supramolecular structure (see below, §3.4.2).

3.3. Ligand geometry

The neutral compounds (I*a*)–(I*e*) all exhibit an unexpected pattern of bond lengths: the detailed comparison of the individual distances with examples retrieved from the CSD and the details of the CSD searches are described by Low *et al.* (2000), and only a brief summary is necessary here. The N1—C2, N2—C2, N1—C6 and N6—C6 bonds in (I*a*)–(I*e*) are always all of rather similar length; the C5—C6 bond is always much longer than expected for a C═C double bond; and the C5—N5 and N5—O5 distances generally differ by less than 0.020 Å: in simple neutral compounds where there is no possibility of significant electronic delocalization these distances normally differ by at least 0.20 Å (Talberg, 1977; Schlemper *et al.*, 1986).

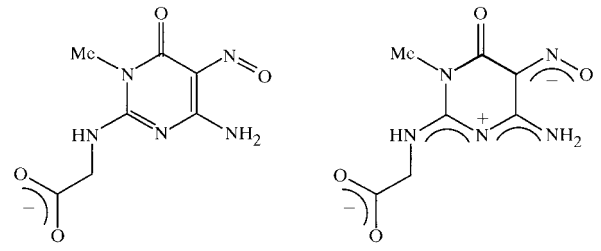

The corresponding geometric parameters for the anions in (1)–(6) (Table 3) exhibit almost all of the same properties. Bond *e* is always short and in the sequence of bonds *g*, *a*, *f*, *h* there is no clear distinction between single C—N and double C═N bonds, such a distinction would be required by form (*A*). In none of the salts described here is bond *a* the shortest in this sequence, as would be expected for form (*A*).

In our previous study (Low *et al.*, 2000), database analysis showed that there were two distinct domains of behaviour for the C-nitroso group in neutral compounds. In one domain there were short O—H···O hydrogen bonds present with O···O distances less than 2.50 Å in which the nitroso O acted as the hydrogen-bond acceptor: in this domain the C—N and N—O distances in the C-nitroso fragment were very similar with the derived parameter $\Delta = |d(\mathrm{C{-}N}) - d(\mathrm{N{-}O})| = 0.020$ Å. In the other domain, where the shortest intermolecular O···O distances involving the nitroso O exceeded 2.66 Å, neutral compounds all had $\Delta > 0.060$ Å. In the neutral compounds (I) (Low *et al.*, 2000) the short-domain O···O distances are associated with H···O distances of 1.71 Å or less, whereas in the long O···O domain the H···O distances all exceed 1.84 Å.

In the present series of compounds, the value of the parameter Δ ranges from 0.041 Å in (3) to 0.066 Å in (5), thus neatly spanning the gap found in neutral species. If (2) and (3), where the nitroso group is ligated to a metal, are excluded from consideration, then the O···O distances for the intermolecular hydrogen bonds having the nitroso O as an acceptor increase in the order (6) < (1) < (4) < (5), while the corresponding values of Δ follow the same order (Tables 3 and 4). While it is implausible to claim a correlation from a sample of only four examples, nonetheless the common ordering is suggestive. Compounds (2) and (3), although their crystal structures do not contain any short hydrogen bonds with the nitroso O as an acceptor [indeed, in (2) there are no hydrogen bonds to this O at all], exhibit the smallest values of Δ in this series. Thus, consistent with the earlier study, an enhanced contribution of the charge separated form (*B*) is associated with either strong intermolecular hydrogen bonding to the nitroso O or with the complexation of the nitroso group to a metal ion, such as Na^+ or K^+. This latter association is particularly significant here since in our earlier modelling studies,

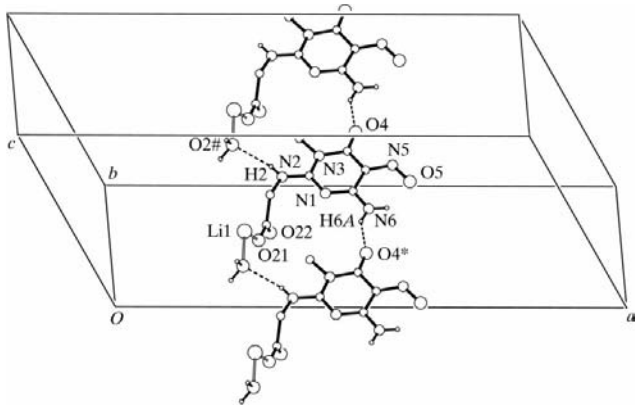

Figure 10
Part of the crystal structure of (1), showing the formation of a chain of $R_2^2(17)$ rings parallel to [010]. Atoms marked with a star (*) or hash (#) are at the symmetry positions $(x, -1+y, z)$ and $(x, 1+y, z)$, respectively.

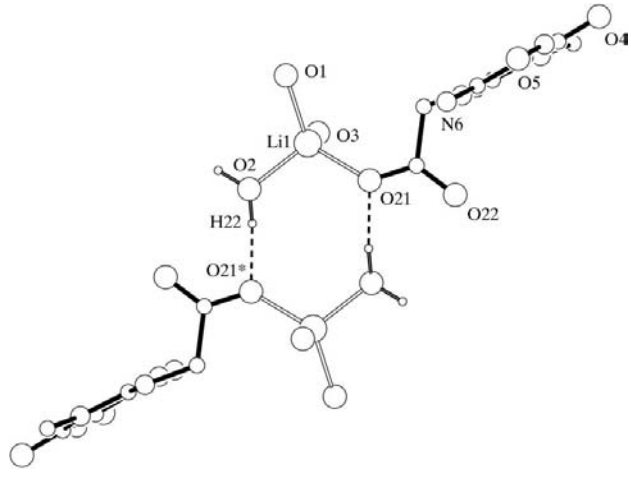

Figure 11
Part of the crystal structure of (1), showing the formation of an $R_2^2(8)$ ring linking a pair of [010] chains. The atom marked with a star (*) is at the symmetry position $(\frac{1}{2}-x, \frac{1}{2}-y, -z)$.

the bonding pattern characteristic of form *B* could be well reproduced by the introduction of a polarizing positive charge adjacent to the nitroso group: this polarization has now been realised experimentally in (2) and (3).

The other aspect of ligand geometry worthy of comment concerns the carboxylate group of the anion L^-. In each of compounds (1), (2) and (3), the two C—O distances within the carboxylate group are not significantly different from one another: only in the Mn complex (4) do these values differ significantly, 1.250 (2) and 1.267 (2) Å. However, the difference between these values in a monodentate carboxylato ligand should be compared with the corresponding values in the Mg compound (5), 1.2442 (17) and 1.2630 (16) Å, and in the Zn compound (6), 1.243 (2) and 1.257 (2) Å, in neither of which is there any direct coordination of the anionic ligand to the metal. Evidently, in all of the compounds reported here, the covalence in the *M*—O(carboxylato) bonds is extremely low.

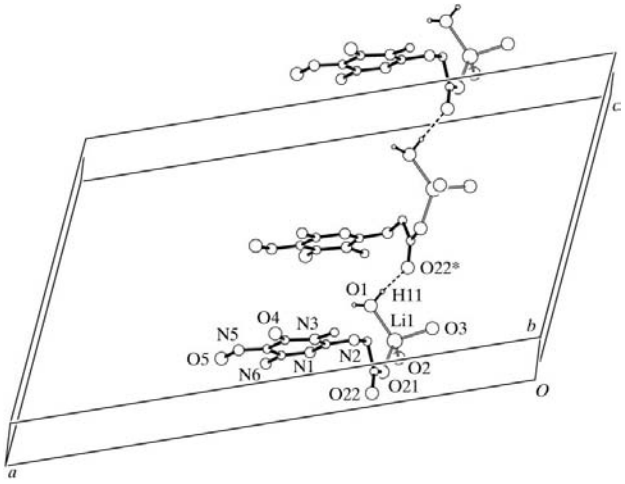

Figure 12
Part of the crystal structure of (1), showing the formation of a *C*(6) chain parallel to [001] linking the [010] chains into (100) sheets. The atom marked with a star (*) is at the symmetry position $(x, 1-y, \frac{1}{2}+z)$.

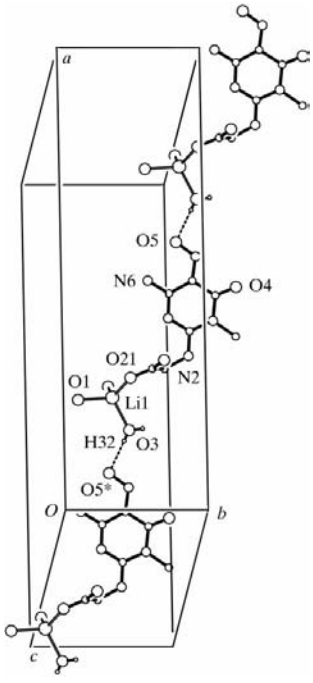

Figure 13
Part of the crystal structure of (1), showing the formation of a *C*(13) chain parallel to [110]. The atom marked with a star (*) is at the symmetry position $(-\frac{1}{2}+x, -\frac{1}{2}+y, z)$.

3.4. Hydrogen bonding

3.4.1. Hydrogen-bond dimensions. The majority of the intermolecular hydrogen bonds in (1), (2), (3) and (4) are of N—H···O and O—H···O types (Table 4). For the N—H···O hydrogen bonds, the extreme values of the N···O distance, 2.796 (2) and 3.187 (2) Å occur in (3) and (2), respectively and, surprisingly, the longest example has an anionic carboxylate O as an acceptor.

Most of the O—H···O hydrogen bonds have carboxylate O as an acceptor and for this category, 12 in all, the O···O distances range from 2.691 (2) Å in (2) to 2.981 (3) Å in (4), with mean value 2.775 Å; the mean O—H···O angle is 168°. Although there are only three examples with nitroso O as an acceptor, the O···O distances in this category range from 2.692 (2) Å in (1) to 2.761 (2) Å in (3) so that the mean distance is slightly shorter than for those having carboxylate acceptors. This is consistent with the extensive polarization of the electronic charge in the nitrosopyrimidine fragments (§3.3). For water and amidic O acceptors, the mean O···O distances are 2.802 Å (five examples) and 2.952 Å (only two examples), respectively: it is noteworthy that the O—H···O angles for the amidic acceptors are 148 and 140°, less than for all the other hydrogen bonds of O—H···O type (Table 4).

3.4.2. Hydrogen-bond motifs. In each of the compounds discussed here, the water molecules all act as double donors in hydrogen bonds, regardless of whether or not the water is directly coordinated to a metal ion. In the organic ligands there is always an intramolecular N—H···O hydrogen bond

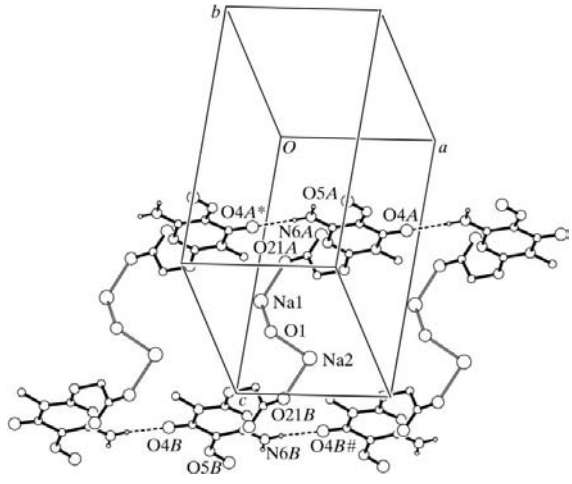

Figure 14
Part of the crystal structure of (2), showing the formation of a hydrogen-bonded molecular ladder parallel to [100]. Atoms marked with a star (*) or hash (#) are at the symmetry positions $(-1+x, y, z)$ and $(1+x, y, z)$, respectively.

formed between amino N6 and the nitroso O5, in an $S(6)$ motif (Bernstein *et al.*, 1995): the other two N—H bonds, one at N2 and one at N6, both engage in the formation of intermolecular N—H···O hydrogen bonds. There are thus many different hydrogen bonds in each of these structures (Table 4), a total of nine in (1), 12 in (2), five in (3) and 13 in (4).

Overall descriptions based on graph-set analyses are thus likely to produce descriptors so complex as to obscure, rather than provide, useful structural insights. We do not therefore discuss in detail all of the hydrogen-bond motifs but, rather, we pick out below just those points at which the hydrogen bonding makes a material difference to the structure defined so far by the metal–ligand coordination, in particular to its overall dimensionality. In (2), in particular, several of the hydrogen bonds simply reinforce the structural motifs established by the metal–ligand coordination.

Compound (1): The metal–ligand coordination generates a finite (zero-dimensional) species $[Li(L)(H_2O)_3]$: eight distinct intermolecular hydrogen bonds link these molecular units into a continuous three-dimensional framework in which each unit forms hydrogen bonds with 12 others. Of the seven O atoms within the $[Li(L)(H_2O)_3]$ unit, all but O1 act as hydrogen-bond acceptors, and the amidic O4 and the carboxylate O22 both act as double acceptors of intermolecular hydrogen bonds.

As is often the case with three-dimensional structures, the descriptive analysis can be much simplified by the identification of a substructure of lower dimensionality (Gregson *et al.*, 2000). In (1) it is convenient to pick out a one-dimensional substructure generated by the two intermolecular N—H···O hydrogen bonds, and then to consider how these one-dimensional units are further linked into a three-dimensional framework by means of the O—H···O hydrogen bonds.

The two N—H···O hydrogen bonds generate by translation a chain of $R_2^2(17)$ rings running parallel to the [010] direction (Fig. 10), and there are eight of these chains running through each unit cell. A single O—H···O hydrogen bond links these chains into pairs: O2 at (x, y, z) is a hydrogen-bond donor, *via* H22, to O21 at $(\frac{1}{2} - x, \frac{1}{2} - y, -z)$ producing a centrosymmetric $R_2^2(8)$ ring (Fig. 11). Two further O—H···O hydrogen bonds suffice to linked the paired chains into a continuous framework. Atom O1 at (x, y, z) acts as a donor, *via* H11, to O22 at $(x, 1 - y, \frac{1}{2} + z)$ so producing a zigzag $C(6)$ chain, running parallel to [001] and generated by the glide plane at $y = 0.5$ (Fig. 12): this increases the dimensionality to two. Finally, O3 at (x, y, z) acts as a donor, *via* H32, to nitroso O5 at $(-\frac{1}{2} + x, -\frac{1}{2} + y, z)$ so producing, by means of the centring translation, a $C(13)$ chain parallel to the [110] direction (Fig. 13). The combination of the paired [010] chains with those along [001] and [110] is sufficient to link all of the molecular $[Li(L)(H_2O)_3]$ units into a single framework. The remaining O—H···O hydrogen bonds reinforce this framework, particularly in the [010] direction, but do not alter its essential character.

Compound (2): In (2) the metal–ligand coordination generates hybrid sheets parallel to $(\bar{1}11)$. The hydrogen bonding, in which four of the N—H bonds and all six of the

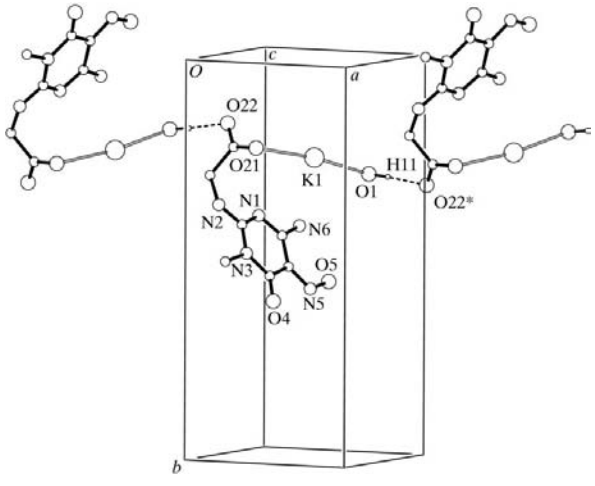

Figure 15
Part of the crystal structre of (3), showing the formation of a $C(6)$ chain parallel to [201]. The atom marked with a star is at the symmetry position $(1 + x, \frac{1}{2} - y, \frac{1}{2} + z)$.

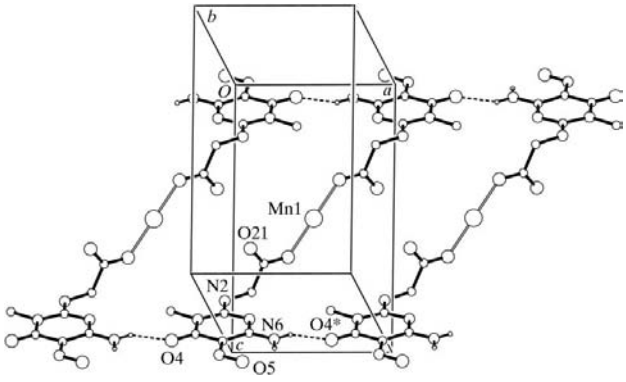

Figure 16
Part of the crystal structure of (4), showing the formation of a molecular ladder parallel to [100] and containing only metal ions and anions. The atom marked with a star (*) is at the symmetry position $(1 + x, y, z)$.

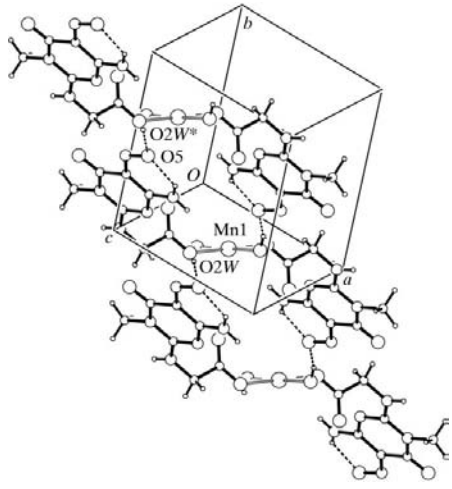

Figure 17
Part of the crystal structure of (4), showing the formation of a molecular ladder parallel to [011]. The atom marked with a star (*) is at the symmetry position $(x, 1 + y, 1 + z)$.

O—H bonds in the asymmetric unit are involved in the formation of intermolecular hydrogen bonds (Table 4), is of some complexity. However, it is only necessary here to pick out those hydrogen bonds which serve to link together the coordination polymer sheets. Paired N—H···O hydrogen bonds link the asymmetric units together to form molecular ladders. N6*A* and N6*B*, each at (x, y, z), act as donors to O4*A* at $(-1+x, y, z)$ and to O4*B* at $(1+x, y, z)$, respectively: each of these interactions generates by translation a $C(6)$ chain running parallel to the [100] direction and these chains form the uprights of the molecular ladder. Paired chains of pyrimidine units are linked by the amino acid/sodium/water components, which act as the rungs of the ladder (Fig. 14). These [100] ladders are sufficient to link all the $(\bar{1}11)$ sheets into a continuous three-dimensional framework.

Compound (3): As in (2), the metal–ligand coordination in (3) generates sheets, in this case parallel to (100). A single O—H···O hydrogen bond is sufficient to link these sheets into a continuous framework. The water O1 at (x, y, z) acts as a hydrogen-bond donor, *via* H11, to carboxylate O22 at $(1+x, \frac{1}{2}-y, \frac{1}{2}+z)$, so producing a $C(6)$ chain (Fig. 15) running parallel to the [201] direction and generated by the glide plane at $y = 0.25$.

Compound (4): The primary metal–ligand coordination in (4) produces a finite (zero-dimensional) molecular complex (Fig. 4), just as found in (1). These molecular units are linked by an extensive series of hydrogen bonds (Table 4) into a single three-dimensional framework. Each of the five independent water molecules acts as a double donor in O—H···O hydrogen bonds and both amino groups in the organic ligand also act as donors in intermolecular N—H···O hydrogen bonds. While there are many *D*, *S* and *R* motifs amongst the very complex hydrogen-bond network, it is sufficient here to draw attention only to the chain-forming motifs along the [100], [010] and [011] directions, which together generate the framework.

Just as in (1) and (2), amino N6 at (x, y, z) acts as a donor to O4 at $(1+x, y, z)$, thus forming a $C(6)$ chain by translation, on this occasion running parallel to [100]. The water O2*W* at (x, y, z) acts as a donor to nitroso O5 at $(x, -1+y, -1+z)$, forming a second chain by translation, a $C(13)$ chain parallel to [011]. Finally, water O4*W* at (x, y, z) acts as a donor to carboxylate O21 at $(x, 1+y, z)$: the resulting chain along [010] involves three different O—H···O hydrogen bonds (Fig. 4) and is of $C_3^3(8)$ type.

As the Mn lies at a centre of inversion, these simple chain motifs are each accompanied by an antiparallel chain generated by the centre of inversion. Thus, in the [100] and [011] directions there are molecular ladders in which the paired antiparallel chains form the uprights, with the Mn at the centre of the rungs (Figs. 16 and 17), while in the [010] direction there is a chain of spiro-linked rings joined at the Mn centres (Fig. 18). Chains of all three types intersect at each Mn, so that all the Mn centres are linked into a single framework.

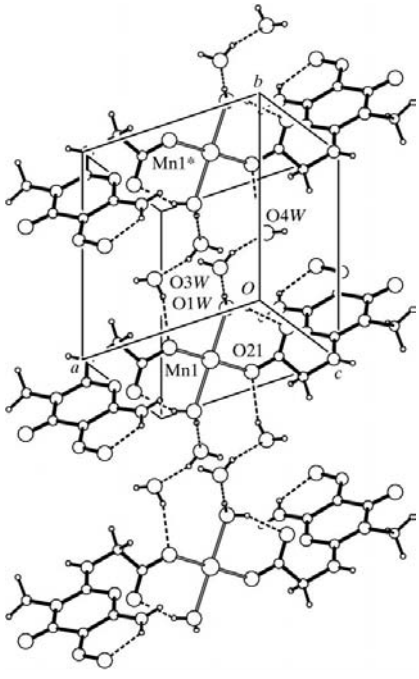

Figure 18
Part of the crystal structure of (4), showing the formation of a chain of spiro-linked $R_6^6(16)$ rings parallel to [010]. The atom marked with a star (*) is at the symmetry position $(x, 1+y, z)$.

4. Concluding comments

The title anion readily forms hydrated neutral complexes with a range of M^+ and M^{2+} cations, and the products exhibit a wide range of structural motifs, both in terms of the metal–ligand coordination and in terms of the hydrogen bonding. Of particular note are the organic inorganic hybrid sheets formed with Na^+ and K^+. The anionic ligand utilized here contains an achiral amino acid residue, but this is, in fact, just the simplest member of an extensive family which are mostly chiral as a consequence of the incorporation of one enantiomeric form of the amino acid (Low *et al.*, 2000). If the chiral ligands in this family form with Na^+ and K^+ hybrid materials similar to those described here, these would necessarily crystallize in non-centrosymmetric space groups, fulfilling one of the requirements for non-linear optical behaviour (Masse *et al.*, 1999; Muthuraman *et al.*, 2000).

X-ray data were collected at the EPSRC X-ray Crystallographic Service, University of Southampton, England, using an Enraf–Nonius Kappa-CCD diffractometer. The authors thank the staff for all their help and advice.

References

Allen, F. H. & Kennard, O. (1993). *Chem. Des. Autom. News*, **8**, 31–37.

Arranz Mascarós, P., Cobo Domingo, J., Godino Salido, M., Gutiérrez Valero, M. D., López Garzón, R. & Low, J. N. (2000). *Acta Cryst.* C**56**, e4–e5.

Arranz Mascarós, P., Godino, M. L., López, R., Cuesta, R., Valenzuela Calahorro, C. & Martín Ramos, D. (1999). *Acta Cryst.* C**55**, 2049–2051.

Bernstein, J., Davis, R. E., Shimoni, L. & Chang, N.-L. (1995). *Angew. Chem. Int. Ed. Engl.* **34**, 1555–1573.
Blessing, R. H. (1995). *Acta Cryst.* A**51**, 33–37.
Blessing, R. H. (1997). *J. Appl. Cryst.* **30**, 421–426.
Brouwer, E. B., Legzdins, P., Rettig, S. J. & Ross, K. J. (1994). *Organometallics*, **13**, 2088–2091.
Clarke, P., Lincoln, S. F. & Tiekink, E. R. T. (1991). *Inorg. Chem.* **30**, 2747–2751.
Duda, A. M., Karaczyn, A., Kozlowski, H., Fritsky, I. O., Glowiak, T., Prisyazhnaya, E. V., Sliva, T. Y. & Swiatek-Kozlowska, J. (1997). *J. Chem. Soc. Dalton Trans.* pp. 3853–3859.
Dutta, S. K., McConville, B. D., Youngs, W. J. & Chaudhury, M. (1997). *Inorg. Chem.* **36**, 2517–2522.
Ferguson, G. (1999). *PRPKAPPA – a WordPerfect5.1 Macro to Formulate and Polish CIF Format Files from the SHELXL97 Refinement of Kappa-CCD Data.* University of Guelph, Canada.
Gack, C. & Klufers, P. (1996). *Acta Cryst.* C**52**, 2972–2975.
Gharbi, A. & Jouini, A. (1996). *Acta Cryst.* C**52**, 1342–1344.
Gonschorek, W. & Kuppers, H. (1975). *Acta Cryst.* B**31**, 1068–1072.
Gregson, R. M., Glidewell, C., Ferguson G. & Lough, A. J. (2000). *Acta Cryst.* B**56**, 39–57.
Helm, F. T., Watson, W. H., Radanovic, D. J. & Douglas, B. E. (1977). *Inorg. Chem.* **16**, 2351–2354.
Herak, R., Manojlovic Muir, L., Djuran, M. I. & Radanovic, D. J. (1985). *J. Chem. Soc. Dalton Trans.* pp. 861–864.
Johnson, C. K. (1976). *ORTEP*II. Report ORNL-5138. Oak Ridge National Laboratory, Tennessee, USA.
Longato, B., Riello, L., Bandoli, G. & Pilloni, G. (1999). *Inorg. Chem.* **38**, 2818–2823.
Low, J. N., Ferguson, G., López, R., Arranz, P., Cobo, J., Melguizo, M., Nogueras, M. & Sánchez, A. (1997). *Acta Cryst.* C**53**, 890–892.
Low, J. N., López, M. D., Arranz Mascarós, P., Cobo Domingo, J., Godino, M. L., López Garzón, R., Gutiérrez, M. D., Melguizo, M., Ferguson, G. & Glidewell, C. (2000). *Acta Cryst.* B**56**, 882–892.
Masse, R., Nicoud, J.-F., Bagieu-Beucher, M. & Bourgogne, C. (1999). *Chem. Phys.* **245**, 365–375.
Minemoto, H., Sonoda, N. & Miki, K. (1992). *Acta Cryst.* C**48**, 737–738.
Muller, G., Maier, G.-M. & Lutz, M. (1994). *Inorg. Chim. Acta*, **218**, 121–131.
Muthuraman, M., Bagieu-Beucher, M., Masse, R., Nicoud, J.-F. & Desiraju, G. R. (1999). *J. Mater. Chem.* **9**, 1471–1474.
Muthuraman, M., Nicoud, J.-F. & Bagieu-Beucher, M. (2000). *Acta Cryst.* C**56**, 1077–1079.
Nonius (1997). *Kappa-CCD Server Software.* Windows 3.11 Version. Nonius BV, Delft, The Netherlands.
Otwinowski, Z. & Minor, W. (1997). *Methods Enzymol.* **276**, 307–326.
Pizzotti, M., Porta, F., Cenini, S., Demartin, F. & Masiocchi, N. (1987). *J. Organomet. Chem.* **330**, 265–278.
Ridouane, F., Sanchez, J., Arzoumanian, H. & Pierrot, M. (1990). *Acta Cryst.* C**46**, 1407–1410.
Schlemper, E. O., Murmann, R. K. & Hussain, M. S. (1986). *Acta Cryst.* C**42**, 1739–1743.
Shannon, R. D. & Prewitt, C. T. (1970). *Acta Cryst.* B**26**, 1046–1047.
Sharma, R. P., Kumar, S., Bashia, K. K. & Tiekink, E. R. T. (1997). *Z. Kristallogr.* **212**, 742–744.
Sheldrick, G. M. (1997*a*). *SHELXS*97. University of Göttingen, Germany.
Sheldrick, G. M. (1997*b*). *SHELXL*97. University of Göttingen, Germany.
Skoog, S. J. & Gladfelter, W. L. (1997). *J. Am. Chem. Soc.* **119**, 11049–11060.
Spek, A. L. (2000). *PLATON.* Utrecht University, The Netherlands.
Talberg, H. J. (1977). *Acta Chem. Scand. Ser. A*, **31**, 485–491.
Town, W. G. & Small, R. W. H. (1973). *Acta Cryst.* B**29**, 1950–1955.
Wilson, A. J. C. (1976). *Acta Cryst.* A**32**, 994–996.
Zavalij, P. Y., Chirayil, T., Whittingham, M. S., Pecharsky, V. K. & Jacobson, R. A. (1997). *Acta Cryst.* C**53**, 170–171.